# Local application of a transcutaneous carbon dioxide paste prevents excessive scarring and promotes muscle regeneration in a bupivacaine-induced rat model of muscle injury

Hirota, Junya ; Hasegawa, Takumi ; Inui, Atsuyuki ; Takeda, Daisuke ; Amano-Iga, Rika ; Yatagai, Nanae ; Saito, Izumi ; Arimoto, Satomi ;…

(Citation)
International Wound Journal,20(4):1151-1159

(Issue Date)
2023-04

(Resource Type)
journal article

(Version)
Version of Record

Received: 15 August 2022 | Revised: 20 September 2022 | Accepted: 27 September 2022

DOI: 10.1111/iwj.13974

ORIGINAL ARTICLE

IWJ WILEY

# Local application of a transcutaneous carbon dioxide paste prevents excessive scarring and promotes muscle regeneration in a bupivacaine-induced rat model of muscle injury

**Junya Hirota**[1] | **Takumi Hasegawa**[1] | **Atsuyuki Inui**[2] | **Daisuke Takeda**[1] | **Rika Amano-Iga**[1] | **Nanae Yatagai**[1] | **Izumi Saito**[1] | **Satomi Arimoto**[1] | **Masaya Akashi**[1]

[1]Department of Oral and Maxillofacial Surgery, Kobe University Graduate School of Medicine, Kobe, Japan

[2]Department of Orthopedic Surgery, Kobe University Graduate School of Medicine, Kobe, Japan

**Correspondence**
Takumi Hasegawa, Department of Oral and Maxillofacial Surgery, Kobe University Graduate School of Medicine, 7-5-1 Kusunoki-cho, Chuo-ku, Kobe 650-0017, Japan.
Email: hasetaku@med.kobe-u.ac.jp

## Abstract

In postoperative patients with head and neck cancer, scar tissue formation may interfere with the healing process, resulting in incomplete functional recovery and a reduced quality of life. Percutaneous application of carbon dioxide ($CO_2$) has been reported to improve hypoxia, stimulate angiogenesis, and promote fracture repair and muscle damage. However, gaseous $CO_2$ cannot be applied to the head and neck regions. Previously, we developed a paste that holds non-gaseous $CO_2$ in a carrier and can be administered transdermally. Here, we investigated whether this paste could prevent excessive scarring and promote muscle regeneration using a bupivacaine-induced rat model of muscle injury. Forty-eight Sprague Dawley rats were randomly assigned to either a control group or a $CO_2$ group. Both groups underwent surgery to induce muscle injury, but the control group received no treatment, whereas the $CO_2$ group received the $CO_2$ paste daily after surgery. Then, samples of the experimental sites were taken on days 3, 7, 14, and 21 post-surgery to examine the following: (1) inflammatory (interleukin [IL]-1β, IL-6), and transforming growth factor (TGF)-β and myogenic (MyoD and myogenin) gene expression by polymerase chain reaction, (2) muscle regeneration with haematoxylin and eosin staining, and (3) MyoD and myogenin protein expression using immunohistochemical staining. Rats in the $CO_2$ group showed higher MyoD and myogenin expression and lower IL-1β, IL-6, and TGF-β expression than the control rats. In addition, treated rats showed evidence of accelerated muscle regeneration. Our study demonstrated that the $CO_2$ paste prevents excessive scarring and accelerates muscle regeneration. This action may be exerted through the induction of an artificial Bohr effect, which leads to the upregulation of MyoD and myogenin, and the downregulation of IL-1β, IL-6, and TGF-β. The paste is

inexpensive and non-invasive. Thus, it may be the treatment of choice for patients with muscle damage.

KEYWORDS

hypoxia, inflammation, scar, transcutaneous $CO_2$, wound healing

**Key Messages**

- we used a bupivacaine-induced rat model of muscle injury and performed gene expression analysis and immunohistochemistry to investigate whether the $CO_2$ paste could prevent excessive scarring and promote muscle regeneration
- forty-eight Sprague Dawley rats that had undergone surgery to induce muscle damage were randomly assigned to the control and $CO_2$ groups. The control group received no treatment, whereas the $CO_2$ group received $CO_2$ paste daily after surgery
- we found that rats treated with the $CO_2$ paste had reduced inflammatory cytokine production and presented evidence of reduced scar formation and accelerated muscle regeneration
- the $CO_2$ paste is inexpensive and non-invasive. Therefore, it may be the treatment of choice for patients with muscle damage. Further research should be conducted to confirm our findings

## 1 | INTRODUCTION

Head and neck cancer has many negative effects on, among others, aesthetics, swallowing, and pronunciation.[1] It often spreads to the cervical lymph nodes and may require neck dissection, which is a reliable method of controlling cervical lymph node metastasis in head and neck cancers. Owing to the development of imaging tests, various techniques have recently been proposed to preserve the function and reduce the dissection range.[2] However, cervical dissection causes a marked decrease in the quality of life due to scar adhesion, which often causes shoulder movement disorders, cervical sensory disorders, and pain after surgery.[3,4] In addition, strong scarring changes due to fibrosis may interfere with early postoperative recurrence diagnosis. Postoperative chemoradiotherapy can also cause further scarring, delay wound healing and hinder reoperation. Injured muscles begin to regenerate quickly, but the healing process is hindered by the formation of scar tissue, which can result in incomplete functional recovery.[5] Therefore, the prevention of scar healing has many advantages for patients.

Carbon dioxide ($CO_2$) therapy has been developed for use in humans and animal models, and its efficacy in treating various conditions, such as limb ischemia and skin disorders, has been evaluated.[6-8] In the field of dermatology, $CO_2$ facial therapy improves the oxygenation of the skin through an artificial Bohr effect.[9] This therapeutic strategy is safe and benefits human health by affecting various biological processes.

We previously showed that 100% $CO_2$ and transcutaneous $CO_2$ absorption enhancing hydrogel ($CO_2$ hydrogel) can accelerate the repair of a fracture and enhance angiogenesis and blood flow.[10] Transcutaneous $CO_2$ therapy also improves blood flow and angiogenesis in skin flaps.[11]Previous studies have used gaseous $CO_2$, but this is not applicable to the head and neck regions. Therefore, we developed a topical cutaneous $CO_2$ paste that generates $CO_2$ within the material by reacting with moisture on the skin's surface and efficiently absorbs $CO_2$ from the skin.[12,13]

Here, our aim was to investigate whether the $CO_2$ paste could prevent excessive scarring and promote muscle regeneration. To that aim, we used a bupivacaine-induced rat model of muscle injury and performed gene expression analysis and immunohistochemistry.

## 2 | MATERIALS AND METHODS

### 2.1 | Animals

A healthy adult male 7-week-old Sprague Dawley rats were procured from the Charles River Laboratories Inc. (Tokyo, Japan). Rats were randomly divided into two groups: the $CO_2$ group ($n = 6$ rats/timepoint) and the control group ($n = 6$ rats/timepoint). All animal

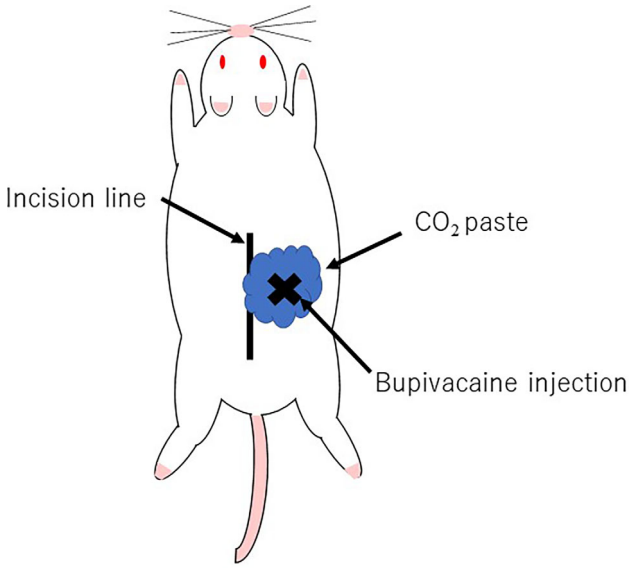


**FIGURE 1** Method of transcutaneous $CO_2$ application of rat scar model

experiments were performed according to the Kobe University Animal Experimentation Regulations (approval number: P171203). The rats were analysed on days 3, 7, 14, and 21 after surgery.

## 2.2 | Bupivacaine-induced muscle injury

Before induction of muscle injury, the rats were anaesthetised using isoflurane (Pfizer) in $O_2$ and injected intraperitoneally with pentobarbital (45 mg/kg body weight; Kyoritsu Seiyaku, Tokyo, Japan). Then, the dorsal skin was shaved, a 2 cm incision was made above the lumbar spine, and 3 mL of bupivacaine (AstraZeneca, London, UK) was intramuscularly injected into the right back muscle using a 20-gauge needle.[14] A suture was attached to the injection site as a mark. The incision was replaced and the skin sutured. We chose this muscle because its position prevents rats from interfering, for example, by biting, with the surgical treatment.

## 2.3 | $CO_2$ paste treatment

The $CO_2$ paste was obtained from $CO_2$Tech (Kobe, Japan) and contained 1,3-butylene glycol, sodium hydrogen carbonate, malic acid, sodium dihydrogen phosphate, alkyl-modified carboxyvinyl polymer, and carboxyvinyl polymer. The backs of the rats in the $CO_2$ group were covered with $CO_2$ paste every day after surgery (Figure 1). The test paste stayed on the wounds for 10 minutes. Control rats underwent muscle damage, and their backs were left untreated. All rats did not receive other special medication.

## 2.4 | Quantitative real-time polymerase chain reaction (PCR)

The mRNA levels of transforming growth factor-β (TGF-β), interleukin-1β (IL-1β), interleukin-6 (IL-6), MyoD, and myogenin were measured. Rats were sacrificed on days 3, 7, 14, and 21 after injury. The experimental sites were dissected and the mRNA from the collected samples was extracted using TRIzol (Invitrogen, Carlsbad, California) and treated using the RNeasy Mini Kit (Qiagen, Valencia, California). Then, cDNA was synthesised (1000 ng of total RNA) using the High-Capacity cDNA Reverse Transcription Kit (Applied Biosystems, Foster City, California). The mRNA levels were quantified using the StepOne Real-Time PCR System (Applied Biosystems). Real-time PCR (20 μL) was performed using 0.5 μM forward primer, 0.5 μM reverse primer, 1 μL of template cDNA, and 10 μL (2×) Power SYBR Green Master Mix (Applied Biosystems). The PCR conditions were as follows: 95°C for 10 minutes, followed by 40 cycles at 95°C for 15 seconds and 60°C for 1 minute. Target gene expression was normalised to β-actin and fold-change was calculated using the $2^{-\Delta\Delta CT}$ method (Applied Biosystems). β-actin, MyoD, myogenin and IL-6 primers were obtained from Invitrogen, and those for TGF-β and IL-1β were procured from Qiagen. The primer sequences were described in Tables 1 and 2.

## 2.5 | Haematoxylin and eosin (H&E) staining

The tissues were fixed in 4% paraformaldehyde and embedded in paraffin wax. Paraffin-embedded 6 μm thick samples were sectioned using a microtome and stained with H&E. The cross-sectional area of the muscle was compared between the groups. Images of the sections were captured using a BZ-X700 microscope at ×400 magnification (Keyence, Osaka, Japan). The cross-sectional area of the muscle was measured in randomly selected identical muscle fields using Image J software (U.S. National Institutes of Health, Bethesda, Maryland).

## 2.6 | Immunohistochemistry

To investigate the expression of myogenic markers, we performed an immunohistochemical assessment of MyoD and myogenin. Formalin-fixed and paraffin-embedded

**TABLE 1** Specific primer sequence for real-time polymerase chain reaction analysis

| Gene name | Primer sequence(5′-3′) | |
|---|---|---|
| β-actin | Fw: GAT GAG ATT GGC ATG GCT TT | Rv: CAC CTT CAC CGT TCC AGT TT |
| MyoD | Fw: ACT ACA GCG GCG ACT CCG ACG CG | Rv: CGC TCC ACT ATG CTG GAC AGG |
| myogenin | Fw: GCC TCC TGC AGTC CAG AGT | Rv: AGT GCA GGT TGT GGG CAT CT |
| IL-6 | Fw: GGT CTT CTG GAG TTC CGT TTC | Rv: GGT CTT GGT CCT TAG CCA CTC |

*Note*: IL-6, Interleukin-6; Fw, Forward primer; Rv, Reverse Primer; A, Adenine; G, Guanine; C, Cytosine; T, Thymine.

**TABLE 2** Primers used for real-time polymerase chain reaction analysis

| Gene name | Primer |
|---|---|
| TGF-β | Rn_Tgfb1_1_SG QuantiTect Primer Assay cat no: QT00187796 |
| IL-1β | Rn_Il1b_1_SG QuantiTect Primer Assay cat no: QT00181657 |

*Note*: TGF-β, transforming growth factor β; IL-1β, Interleukin-1β.

muscle tissue were pretreated with proteinase K, quenched with 0.05% $H_2O_2$, and incubated overnight at 4°C in Can Get Signal Immunostain Solution A (Toyobo, Osaka, Japan) with the following primary antibodies: mouse anti-MyoD antibody (Santa Cruz Biotechnology, sc-32 758, 1:100) and mouse anti-myogenin antibody (Santa Cruz Biotechnology, sc-52 903, 1:100). Following washes twice with Phosphate Buffered Saline, the sections were incubated with peroxidase-conjugated anti-mouse antibody (Histofine Simplestain MAX-PO; Nichirei, Tokyo, Japan; code 424131) for 30 minutes. Following adequate diaminobenzidine staining and counterstaining with haematoxylin, tissue images were acquired using a fluorescence microscope BZ-X700 (Keyence) (×400), and the positive area was automatically quantified using the Hybrid Cell Count BZ-H3C software (Keyence).

## 2.7 | Statistical analysis

Data collection and statistical analyses were performed using Excel 2012 (Social Survey Research Information Co., Ltd., Tokyo, Japan). Data are presented as mean ± SD. Comparisons between the two groups were performed using the Mann–Whitney *U*-test. Statistical significance was set at $P < .05$.

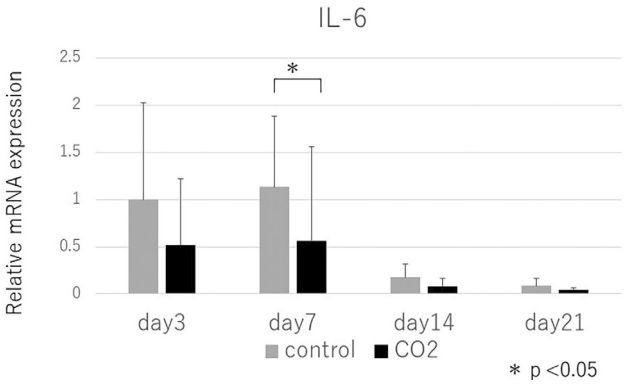


**FIGURE 2** Relative mRNA expression of IL-6. The mRNA expression of IL-6 on days 3, 7, 14, and 21 was evaluated using quantitative real-time PCR (*$P$<.05)

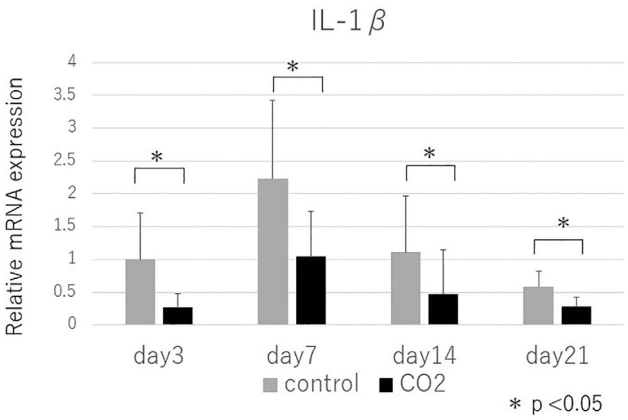


**FIGURE 3** Relative mRNA expression of IL-1β. The mRNA expression of IL-1β on days 3, 7, 14, and 21 was evaluated using quantitative real-time PCR (*$P$<.05)

# 3 | RESULTS

## 3.1 | Gene expression profiles

The PCR results showed that the expression levels of IL-6 (Figure 2, day 7) and IL-1β (Figure 3, all days analysed) were significantly lower in the $CO_2$ group than in the control group ($P < .05$). The expression of TGF-β on day 3 was significantly higher in the $CO_2$ group than in the control group (Figure 4); however, its expression on Day 21 was significantly lower in the $CO_2$ group than in the control group. The expression of MyoD (Figure 5; days 3 and 7) was significantly higher in the $CO_2$ group than in the control group ($P < .05$). Figure 6 shows the expression of myogenin.

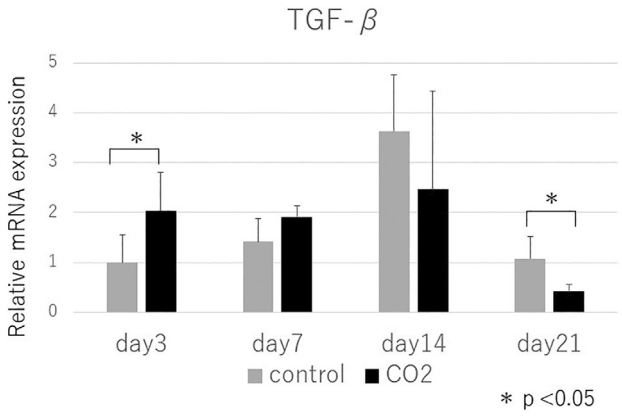


**FIGURE 4** Relative mRNA expression of TGF-β. The mRNA expression of TGF-β on days 3, 7, 14, and 21 was evaluated using quantitative real-time PCR (*$P$<.05)

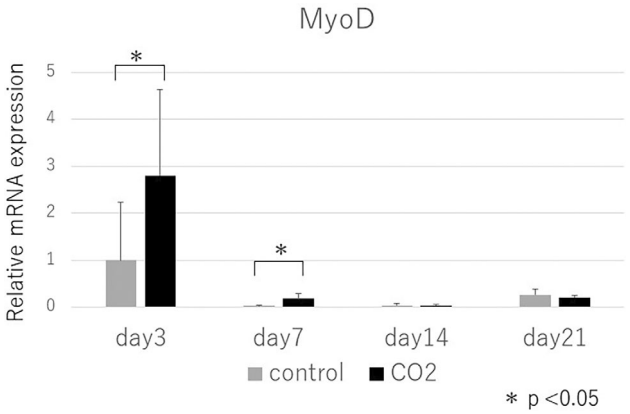


**FIGURE 5** Relative mRNA expression of myogenin. The mRNA expression of myogenin on days 3,7,14, and 21 was evaluated using quantitative real-time PCR (*$P$<.05)

## 3.2 | H&E staining

Figure 7A shows the H&E-stained sections of scars from the two groups on different days. Many inflammatory cells were observed in both groups on day 3, and muscle fibres gradually appeared from day 7 onwards. Although the number and size of myotubes increased and were replaced by newly regenerated fibres in both groups, the $CO_2$ group had more muscle fibres than the control group. Moreover, the number of muscle fibres was higher on day 14 than on day 7, and this increase was more prominent in the $CO_2$ group. The scars disappeared and were almost replaced by muscle fibres on day 21, with no apparent differences between the groups. Figure 7B shows the measured cross-sectional area of each expressed muscle fibre. The cross-sectional area of the muscle in both groups increased as the days passed, and

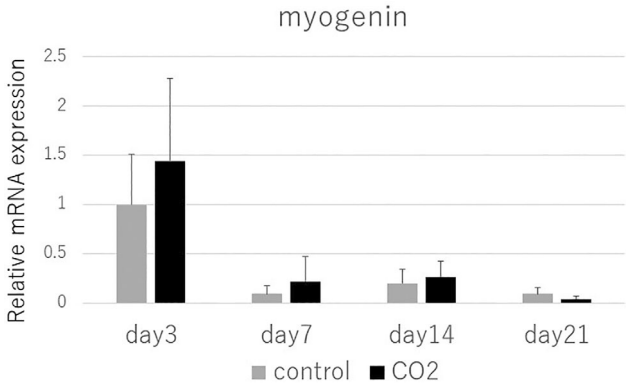


**FIGURE 6** Relative mRNA expression of MyoD. The mRNA expression of MyoD on days 3, 7, 14, and 21 was evaluated using quantitative real-time PCR (*$P$<.05)

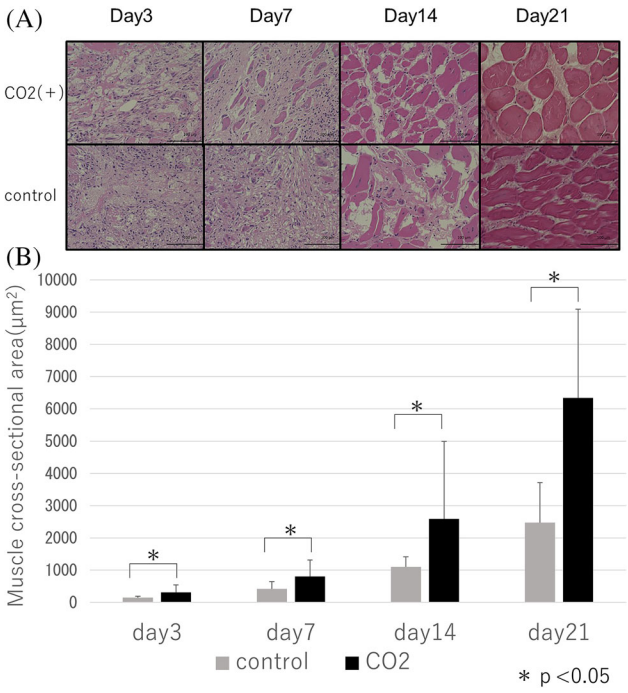


**FIGURE 7** A, H&E staining. H&E histological observation of healing in both groups on 3, 7, 14, and 21 days after muscle injury at ×400 (scale bar = 100 μm). B, Muscle fibre cross-sectional area (μm$^2$) on days 3, 7, 14, and 21 after injury (*$P$ < .05, n = 7)

was significantly larger in the $CO_2$ group than in the control group ($P$ < .05).

## 3.3 | Immunohistochemical analysis

MyoD (Figure 8A and Figure 8B) and myogenin (Figure 9A and Figure 9B) protein levels in the muscle were assessed using immunohistochemistry. In the $CO_2$

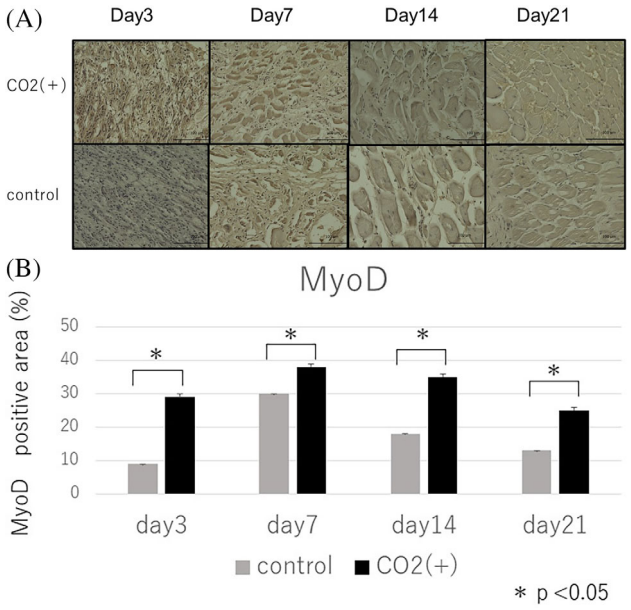


FIGURE 8 A, Immunohistochemical staining of MyoD. Immunohistochemical staining of MyoD during the healing process in both groups on 3, 7, 14, and 21 days after muscle injury at ×400 (scale bar = 100 μm). B, MyoD quantitative immunohistochemical analysis of the primary antibody positive area ratio (*$P$<.05)

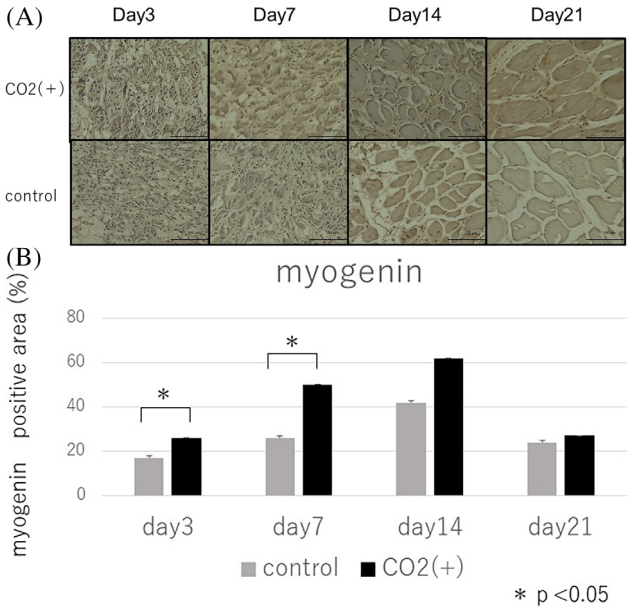


FIGURE 9 A, Immunohistochemical staining of myogenin. Immunohistochemical staining of myogenin during healing process in both groups on 3, 7, 14, and 21 days after muscle injury at ×400 (scale bar = 100 μm). B, Myogenin quantitative immunohistochemical analysis of the primary antibody positive area ratio (*$P$<.05)

group, a significant number of MyoD- and myogenin-positive cells were observed around the regenerated myofibers ($P < .05$). The immunohistochemistry results were elevated in the $CO_2$ group, similar to real-time PCR.

## 4 | DISCUSSION

Gaseous $CO_2$ is used in the treatment of different conditions. $CO_2$ therapy involves transdermal absorption of $CO_2$, which increases vasodilation and blood flow via the Bohr effect, in turn increasing the partial pressure of oxygen in tissues. Previously, we showed that percutaneous administration of $CO_2$ can produce an artificial Bohr effect by increasing the $O_2$ pressure in the tissue upon $CO_2$ absorption.[10] Increased blood flow causes shear stress in endothelial cells, leading to enhanced expression of endothelial nitric oxide synthase (eNOS) in vascular endothelial cells. eNOS plays a major role in many physiological functions, such as the regulation of vascular tone.[15] Upregulation of eNOS expression enhances the expression of VEGF, resulting in angiogenesis in skeletal muscle.[16,17] In addition, we previously demonstrated that $CO_2$ accelerates muscle regeneration by promoting neovascularization through the upregulation of PGC-1α and VEGF.[18] Although conventional methods using gaseous $CO_2$ have many applications, they cannot be applied to the head and neck areas. To overcome this limitation, we developed the $CO_2$ paste and investigated whether this paste can reduce scarring and promote muscle regeneration. To assess this, we used a bupivacaine-induced rat model of muscle injury and performed gene expression analysis and immunohistochemistry.

In summary, we found that rats treated with the $CO_2$ paste had reduced inflammatory cytokine production and presented evidence of reduced scar formation and accelerated muscle regeneration.

Bupivacaine is widely used in the study of morphological changes associated with muscle diseases. Intramuscular injection of bupivacaine causes rapid necrosis of muscle fibres and decreased contractility, leaving the basement membrane, nerves, and blood vessels intact. Furthermore, the injury regenerates completely after the rapid degeneration of skeletal muscle.[19-21] In animal models, skeletal muscle injury consists of three distinct stages.[22] The initial stage is characterised by necrosis of the muscle tissue, degeneration, and an inflammatory response at the site of injury. It involves the invasion of inflammatory cells into the damaged area. Inflammation is an important first step in the wound healing process and is closely related to scar formation. However, chronic and continuous inflammation stimulates the secretion of inflammatory cytokines, leading to excessive scar formation.[23] Therefore, it is important to reduce the inflammatory reaction at an appropriate time point to prevent

excessive scar formation. The second stage involves muscle regeneration and usually starts 7 to 10 days after the injury, reaching its peak approximately 2 weeks after the injury. Therefore, promoting muscle regeneration and preventing fibrosis within 2 weeks after muscle injury is critical for successful treatment, as scar tissue grows over time. Scar formation interferes with the normal muscle healing process and prevents the complete regeneration of muscle tissue.[5,24]

One of the most potent fibrosis-promoting cytokines is TGF-β.[25] TGF-β is implicated in the pathogenesis of fibrosis in most organs, including skeletal muscle.[26] Antagonising TGF-β signalling inhibits fibrosis and promotes muscle regeneration.[5,27] Here, H&E staining at Day 14 revealed that the $CO_2$ group had less fibrous tissue and increased muscle fibre regeneration. The PCR results showed that TGF-β was elevated in the early stages of muscle injury, causing an inflammatory response. In the $CO_2$ group, TGF-β expression was lower than that in the control group during the second half of the experiment, suggesting that this may have led to reduced scarring. In a previous study, $CO_2$ therapy was shown to reduce TGF-β1 protein levels in joint capsules associated with fibrosis and improve the passive range of motion in a rat model.[28] Here, the $CO_2$ paste significantly prevented fibrosis during muscle regeneration, which was likely due to the early downregulation of TGF-β, a major trigger of the fibrosis cascade. In addition, fibrin induces the expression of inflammatory chemokines and cytokines that promote muscle degeneration, such as IL-6 and IL-1β.[29] IL-1β induces fibroblast activation and collagen production through a TGF-β-dependent mechanism.[30] Hypoxia induces inflammation and increases the levels of pro-inflammatory cytokines (IL-6) and C-reactive protein.[31,32] In this study, the expression of IL-6 (Day 7) and IL-1β (days 3, 7, 14, and 21) was lower in the $CO_2$ group than in the control group. Therefore, the $CO_2$ paste may have accelerated muscle repair by preventing excessive inflammatory cytokine production and improving hypoxia. Albes et al[33] concluded that low-level laser therapy may result in reduced IL-6 mRNA expression, thus providing a protective effect that minimises muscle damage by weakening the inflammatory process during muscle repair. Song et al[34] reported that low-level laser therapy reduces IL-1β levels, suppresses inflammation and decreases skeletal muscle damage in a mouse model of muscle injury. Otis et al[35] showed that high cytokine levels (IL-1β, TNF-α, IFN-γ, etc.) mitigate or disable myoblast proliferation.

MyoD, a basic helix–loop–helix transcription factor belonging to the myogenic regulatory factor family (MRF),[36] and myogenin are induced during myoblast and myotube myogenic differentiation and are considered markers of muscle growth and hypertrophy.[19,22,37] In the early stages of muscle regeneration, inflammatory responses, and necrosis of damaged tissue lead to the activation and proliferation of adult satellite cells,[38,39] which repair the damaged area through the cell cycle, division, differentiation, and fusion with myofibers.[38,40] Furthermore, it has been reported that MyoD is rapidly expressed within 12 hours after injury.[38] Subsequently, increased expression of secondary MRFs, such as myogenin, induces terminal differentiation, and myoblasts eventually differentiate into skeletal muscle.[39]

Nakasa et al[22] demonstrated that local injection of muscle-specific microRNAs promotes muscle regeneration in a rat skeletal muscle injury model by downregulating TGF-β and upregulating MyoD and myogenin. Several investigators have reported a significant relationship between PGC-1α and MyoD.[41] In previous studies, they reported that the transcutaneous application of $CO_2$ using $CO_2$ hydrogel enhances muscle regeneration and fracture healing.[18,42,43] In this study, we reported that transcutaneous application of $CO_2$ paste results in the upregulation of MyoD and myogenin and the activation of myogenesis, which may be involved in the upregulation of mitochondrial biogenesis. In this study, PCR analyses revealed that the expression of MyoD and myogenin was upregulated on Day 3 after muscle injury in the $CO_2$ group. Immunohistochemical staining for MyoD and myogenin showed that their expression increased during the active phase of muscle regeneration. In other words, our experiments revealed that the $CO_2$ paste can accelerate muscle regeneration.

## 5 | CONCLUSIONS

In conclusion, our study demonstrates that the $CO_2$ paste prevents excessive scarring and accelerates muscle regeneration. This may be due to the induction of an artificial Bohr effect, which leads to the upregulation of MyoD and myogenin, and the downregulation of IL-1β, IL-6, and TGF-β. The $CO_2$ paste is inexpensive and non-invasive. Therefore, it may be the treatment of choice for patients with muscle damage. Further research should be conducted to confirm our findings.

### ACKNOWLEDGEMENTS

We are thankful to Minako Nagata, Maya Yasuda and Kyoko Tanaka for their expert technical assistance. We would like to thank Editage (www.editage.com) for English language editing.

### CONFLICT OF INTEREST

The authors declare that there is no conflict of interest regarding the publication of this paper.

## DATA AVAILABILITY STATEMENT

The data that support the findings of this study are available from the corresponding author upon reasonable request.

## REFERENCES


1. Shah S, Har-el G, Rosenfeld RM. Short-term and long-term quality of life after neck dissection. *Head Neck*. 2001;23(11):954-961.
2. Nibu K, Ebihara Y, Ebihara M, et al. Quality of life after neck dissection: a multicenter longitudinal study by the Japanese Clinical Study Group on standardization of treatment for lymph node metastasis of head and neck cancer. *Int J Clin Oncol*. 2010;15(1):33-38.
3. Paul Van Wilgen C, Dijkstra PU, van der Laan BFAM, Plukker JT, Roodenburg JLN. Morbidity of the neck after head and neck cancer therapy. *Head Neck*. 2004;26:785-791.
4. Kamel FH, Basha M, Alsharidah A, Hewidy IM, Ezzat M, Aboelnour NH. Efficacy of extracorporeal shockwave therapy on cervical myofascial pain following neck dissection surgery: a randomized controlled trial. *Ann Rehabil Med*. 2020;44(5):393-401.
5. Huard J, Li Y, Fu FH. Muscle injuries and repair: current trends in research. *J Bone Joint Surg Am*. 2002;84(5):822-832.
6. Yamamoto N, Hashimoto M. Immersion in CO2-rich water containing NaCl diminishes blood pressure fluctuation in anesthetized rats. *Int J Biometeorol*. 2007;52(2):109-116.
7. Brandi C, D'Aniello C, Grimaldi L, et al. Carbon dioxide therapy in the treatment of localized adiposities: clinical study and histopathological correlations. *Aesthetic Plast Surg*. 2001;25(3):170-174.
8. Brandi C, Grimaldi L, Nisi G, et al. The role of carbon dioxide therapy in the treatment of chronic wounds. *In Vivo*. 2010;24(2):223-226.
9. Seidel R, Moy R. Effect of carbon dioxide facial therapy on skin oxygenation. *J Drugs Dermatol*. 2015;14(9):976-980.
10. Sakai Y, Miwa M, Oe K, et al. A novel system for transcutaneous application of carbon dioxide causing an "artificial Bohr effect " in the human body. *PLoS One*. 2011;6(9):e24137.
11. Saito I, Hasegawa T, Ueha T, et al. Effect of local application of transcutaneous carbon dioxide on survival of random-pattern skin flaps. *J Plast Reconstr Aesthet Surg*. 2018;71(11):1644-1651.
12. Takeda D, Hasegawa T, Ueha T, et al. Transcutaneous carbon dioxide induces mitochondrial apoptosis and suppresses metastasis of oral squamous cell carcinoma in vivo. *PLoS One*. 2014;9(7):e100530.
13. Yatagai N, Hasegawa T, Amano R, et al. Transcutaneous carbon dioxide decreases immunosuppressive factors in squamous cell carcinoma in vivo. *Biomed Res Int*. 2021;2021:5568428.
14. Cianforlini M, Grassi M, Coppa V, et al. Skeletal muscle repair in a rat muscle injury model: the role of growth hormone(GH) injection. *Eur Rev Med Pharmacol Sci*. 2020;24(16):8566-8572.
15. Huang PL, Huang Z, Mashimo H, et al. Hypertension in mice lacking the gene for endothelial nitric oxide synthase. *Nature*. 1995;377(6546):239-242.
16. Oe K, Ueha T, Sakai Y, et al. The effect of transcutaneous application of carbon dioxide (CO2) on skeletal muscle. *Biochem Biophys Res Commun*. 2011;407(1):148-152.
17. Irie H, Tatsumi T, Takamiya M, et al. Carbon dioxide-rich water bathing enhances collateral blood flow in ischemic hindlimb via mobilization of endothelial progenitor cells and activation of NO-cGMP system. *Circulation*. 2005;111(12):1523-1529.
18. Akahane S, Sakai Y, Ueha T, et al. Transcutaneous carbon dioxide application accelerates muscle injury repair in rat models. *Int Orthop*. 2017;41(5):1007-1015.
19. Zammit PS. Function of the myogenic regulatory factors Myf5, MyoD, Myogenin and MRF4 in skeletal muscle, satellite cells and regenerative myogenesis. *Semin Cell Dev Biol*. 2017;72:19-32.
20. Benoit PW, Belt WD. Degeneration and regeneration of skeletal muscle after treatment with a local anaesthetic, bupivacaine(Marcaine). *J Anat*. 1970;107(3):547-556.
21. Sakakima H, Kamizono T, Matsuda F, Izumo K, Ijiri K, Yoshida Y. Midkine and its receptor in regenerating rat skeletal muscle after bupivacaine injection. *Acta Histochem*. 2006;108(5):357-364.
22. Nakasa T, Ishikawa M, Shi M, Shibuya H, Adachi N, Ochi M. Acceleration of muscle regeneration by local injection of muscle-specific microRNAs in rat skeletal muscle injury model. *J Cell Mol Med*. 2010;14(10):2495-2505.
23. Jeong W, Yang CE, Roh TS, Kim JH, Lee JH, Lee WJ. Scar prevention and enhanced wound healing induced by polydeoxyribonucleotide in a rat incisional wound-healing model. *Int J Mol Sci*. 2017;18(8):1-12.
24. Assis L, Moretti AI, Abrahão TB, de Souza HP, Hamblin MR, Parizotto NA. Low-level laser therapy (808 nm) contributes to muscle regeneration and prevents fibrosis in rat tibialis anterior muscle after cryolesion. *Lasers Med Sci*. 2013;28(3):947-955.
25. Mann CJ, Perdiguero E, Kharraz Y, et al. Aberrant repair and fibrosis development in skeletal muscle. *Skelet Muscle*. 2011;1(1):1-20.
26. Ismaeel A, Kim JS, Kirk JS, Smith RS, Bohannon WT, Koutakis P. Role of transforming growth factor-β in skeletal muscle fibrosis: a review. *Int J Mol Sci*. 2019;20(10):2446.
27. Kollias HD, McDermott JC. Transforming growth factor-β and myostatin signaling in skeletal muscle. *J Appl Physiol*. 2008;104(3):579-587.
28. Inoue S, Moriyama H, Wakimoto Y, et al. Transcutaneous application of carbon dioxide improves contractures after immobilization of rat knee joint. *Phys Ther Res*. 2020;23(2):113-122.
29. Vidal B, Serrrano AL, Tjwa M, et al. Fibrinogen drives dystrophic muscle fibrosis via a TGFβ/alternative macrophage activation pathway. *Genes Dev*. 2008;22(13):1747-1752.
30. Vesey DA, Cheung C, Cuttle L, Endre Z, Gobe G, Johnson DW. Interleukin-1beta stimulates human renal fibroblast proliferation and matrix protein production by means of a transforming growth factor-beta-dependent mechanism. *J Lab Clin Med*. 2002;140(5):342-350.
31. Eltzschig HK, Carmeliet P. Hypoxia and inflammation. *N Engl J Med*. 2011;364(7):656-665.
32. Hartmann G, Tachop M, Fischer R, et al. High altitude increases circulating interleukin-6, interleukin-1 receptor antagonist and C-reactive protein. *Cytokine*. 2000;12(3):246-252.

33. Alves AN, Ribeiro BG, Fernandes KPS, et al. Comparative effects of low-level laser therapy pre- and post-injury on mRNA expression of MyoD, myogenin, and IL-6 during the skeletal muscle repair. *Lasers Med Sci*. 2016;31(4):679-685.
34. Song DH, Kim MH, Lee YT, Lee JH, Kim KA, Kim SJ. Effect of high frequency electromagnetic wave stimulation on muscle injury in a rat model. *Injury*. 2018;49(6):1032-1037.
35. Otis JS, Niccoli S, Hawdon N, et al. Pro-inflammatory mediation of myoblast proliferation. *PLoS One*. 2014;9(3):1-10.
36. Sakuma K, Watanabe K, Sano M, Uramoto I, Sakamoto K, Totsuka T. The adaptive response of MyoD family proteins in overloaded, regenerating and denervated rat muscles. *Biochim Biophys Acta*. 1999;1428(2–3):284-292.
37. Gomes AR, Soares AG, Peviani S, Nascimento RB, Moriscot AS, Salvini TF. The effect of 30 minutes of passive stretch of the rat soleus muscle on the myogenic differentiation, myostatin, and atrogin-1 gene expressions. *Arch Phys Med Rehabil*. 2006;87(2):241-246.
38. Rantanen J, Hurme T, Lukka R, Heino J, Kalimo H. Satellite cell proliferation and the expression of myogenin and desmin in regenerating skeletal muscle: evidence for two different populations of satellite cells. *Lab Invest*. 1995;72(3):341-347.
39. Chargé SBP, Rudnicki MA. Cellular and molecular regulation of muscle regeneration. *Physiol Rev*. 2004;84(1):209-238.
40. Le GF, Rudnicki MA. Skeletal muscle satellite cells and adult myogenesis. *Curr Opin Cell Biol*. 2007;19(6):628-633.
41. Amat R, Planavila A, Chen SL, Iglesias R, Giralt M, Villarroya F. SIRT1 controls the transcription of the peroxisome proliferator-activated receptor-gamma Co-activator-1alpha (PGC-1alpha) gene in skeletal muscle through the PGC-1alpha autoregulatory loop and interaction with MyoD. *J Biol Chem*. 2009;284(33):21872-21880.
42. Koga T, Niikura T, Lee SY, et al. Topical cutaneous CO2 application by means of a novel hydrogel accelerates fracture repair in rats. *J Bone Joint Surg Am*. 2014;96(24):2077-2084.
43. Nishimoto H, Inui A, Ueha T, et al. Transcutaneous carbon dioxide application with hydrogel prevents muscle atrophy in a rat sciatic nerve crush model. *J Orthop Res*. 2018;36(6):1653-1658.

**How to cite this article:** Hirota J, Hasegawa T, Inui A, et al. Local application of a transcutaneous carbon dioxide paste prevents excessive scarring and promotes muscle regeneration in a bupivacaine-induced rat model of muscle injury. *Int Wound J*. 2022;1-9. doi:10.1111/iwj.13974